Functional redundancy of mitochondrial enoyl-CoA isomerases in the oxidation of unsaturated fatty acids

Michel van Weeghel,* Heleen te Brinke,* Henk van Lenthe,* Wim Kulik,* Paul E. Minkler,‡ Maria S. K. Stoll,‡ Jörn Oliver Sass,‖,¶ Uwe Janssen,# Wilhelm Stoffel, K. Otfried Schwab,‖ Ronald J. A. Wanders,*,† Charles L. Hoppel,‡,§ and Sander M. Houten*,†,1**

*Department of Clinical Chemistry, Laboratory Genetic Metabolic Diseases, and †Department of Pediatrics, Emma Children's Hospital, Academic Medical Center, University of Amsterdam, Amsterdam, The Netherlands; ‡Department of Pharmacology and §Department of Medicine, Case Western Reserve University School of Medicine, Cleveland, Ohio, USA; ‖Center for Children's Hospital in Freiburg, Freiburg, Germany; ¶Department of Clinical Chemistry and Biochemistry, University Children's Hospital Zürich, Zürich, Switzerland; #Miltenyi Biotec GmbH, Bergisch Gladbach, Germany; **Institute of Biochemistry, Center of Molecular Medicine Cologne, Cluster of Excellence, Cellular Stress Response in Aging Related Diseases (CECAD), University of Cologne, Germany

ABSTRACT **Mitochondrial enoyl-CoA isomerase (ECI1) is an auxiliary enzyme involved in unsaturated fatty acid oxidation. In contrast to most of the other enzymes involved in fatty acid oxidation, a deficiency of ECI1 has yet to be identified in humans. We used wild-type (WT) and Eci1-deficient knockout (KO) mice to explore a potential presentation of human ECI1 deficiency. Upon food withdrawal, Eci1-deficient mice displayed normal blood β-hydroxybutyrate levels (WT 1.09 mM *vs.* KO 1.10 mM), a trend to lower blood glucose levels (WT 4.58 mM *vs.* KO 3.87 mM, $P=0.09$) and elevated blood levels of unsaturated acylcarnitines, in particular C12:1 acylcarnitine (WT 0.03 μM *vs.* KO 0.09 μM, $P<0.01$). Feeding an olive oil-rich diet induced an even greater increase in C12:1 acylcarnitine levels (WT 0.01 μM *vs.* KO 0.04 μM, $P<0.01$). Overall, the phenotypic presentation of Eci1-deficient mice is mild, possibly caused by the presence of a second enoyl-CoA isomerase (Eci2) in mitochondria. Knockdown of Eci2 in Eci1-deficient fibroblasts caused a more pronounced accumulation of C12:1 acylcarnitine on incubation with unsaturated fatty acids (12-fold, $P<0.05$). We conclude that Eci2 compensates for Eci1 deficiency explaining the mild phenotype of Eci1-deficient mice. Hypoglycemia and accumulation of C12:1 acylcarnitine might be diagnostic markers to identify ECI1 deficiency in humans.—van Weeghel, M., te Brinke, H., van Lenthe, H., Kulik, W., Minkler, P. E., Stoll, M. S. K., Sass, J. O., Janssen, U., Stoffel, W., Schwab, O. K., Wanders, R. J. A., Hoppel, C. L., Houten, S. M. Functional redundancy of mitochondrial enoyl-CoA isomerases in the oxidation of unsaturated fatty acids. *FASEB J.* 26, 4316–4326 (2012). www.fasebj.org**

Key Words: mouse models · inherited metabolic disease

Mitochondrial fatty acid β-oxidation (FAO) is the most important pathway for the degradation of saturated and unsaturated fatty acids. The β-oxidation cycle of fatty acids consists of 4 sequential reactions: dehydrogenation, hydration, a second dehydrogenation, and thiolytic cleavage. Every cycle shortens the acyl-CoA by 2 carbon atoms and generates an acetyl-CoA. In addition to the set of enzymes involved in this β-oxidation cycle, the degradation of unsaturated fatty acids requires the obligatory participation of a set of 3 auxiliary enzymes: the 2,4-dienoyl-CoA reductase (DECR), the $\Delta^{3,5},\Delta^{2,4}$-dienoyl-CoA isomerase, and the Δ^{3},Δ^{2}-enoyl-CoA isomerase (ECI) (1). An important reason for this phenomenon is that the first dehydrogenase in the oxidation cycle has a *trans*-2-enoyl-CoA intermediate as the product and therefore cannot directly metabolize the *cis*-3-enoyl-CoA configuration of unsaturated fatty acyl-CoAs. The combined set of 3 auxiliary enzymes can position different combinations of double bonds in the acyl-CoA to the *trans*-2 config-

Abbreviations: ACN, acetonitrile; BSA, bovine serum albumin; DECR, 2,4-dienoyl-CoA reductase; ECI, Δ^{3},Δ^{2}-enoyl-CoA isomerase; EHHADH, enoyl-CoA hydratase/3-hydroxyacyl CoA dehydrogenase; FAO, fatty acid β-oxidation; GDH, glutamate dehydrogenase; HPLC, high-pressure liquid chromatography; KO, knockout; LCAD, long-chain acyl-CoA dehydrogenase; MS/MS, tandem mass spectrometry; PPARα, peroxisome proliferator-activated receptor α; UPLC, ultra-performance liquid chromatography; VLCAD, very long chain acyl-CoA dehydrogenase; WT, wild type

[1] Correspondence: Laboratory Genetic Metabolic Diseases (F0-222), Academic Medical Center, University of Amsterdam, Meibergdreef 9, 1105 AZ Amsterdam, The Netherlands. E-mail: s.m.houten@amc.uva.nl

doi: 10.1096/fj.12-206326

This article includes supplemental data. Please visit *http://www.fasebj.org* to obtain this information.

0892-6638/12/0026-4316 © FASEB

uration, allowing reentrance into the β-oxidation cycle (2). The action of these three auxiliary enzymes is illustrated by the metabolism of oleic acid (**Fig. 1*A***) and linoleic acid (Fig. 1*B*). Oleoyl-CoA (*cis*-9-C18:1-CoA) is converted by 2 cycles of β-oxidation to *cis*-5-C14:1-CoA, the substrate for long-chain acyl-CoA dehydrogenase (LCAD) that further converts it into *trans*-2,*cis*-5-C14:2-CoA. From there on, the oxidation can occur *via* an isomerase- or a reductase-dependent pathway, but the major route is *via* the isomerase-dependent pathway (85%) (3). For the reductase-dependent pathway, the auxiliary enzymes $\Delta^{3,5},\Delta^{2,4}$-dienoyl-CoA isomerase and DECR are needed. Both routes require the involvement of ECI (ref. 3 and Fig. 1*A*). ECI catalyzes the conversion of the double bond in *cis*-3-enoyl-CoA or *trans*-3-enoyl-CoA to *trans*-2-enoyl-CoA (Fig. 1*A*). In the reductase-dependent pathway, ECI is also responsible for the reverse reaction in which the *trans*-2,*cis*-5-C14:2-CoA is converted into *trans*-3,*cis*-5-C14:2-CoA (Fig. 1*A*). Linoleoyl-CoA (*cis*-9,12-C18:2-CoA) is converted by 3 cycles of β-oxidation to *cis*-3,6-C12:2-CoA. From there on, the auxiliary enzymes ECI and DECR are needed (Fig. 1*B* and ref. 2).

Different ECIs have been purified, cloned, and characterized (4–7). ECI can be present either as a monofunctional protein or as an integral part of the L-bifunctional protein enoyl-CoA hydratase/3-hydroxyacyl CoA dehydrogenase (EHHADH), also known as multifunctional β-oxidation enzyme type 1 (8), but in all cases,

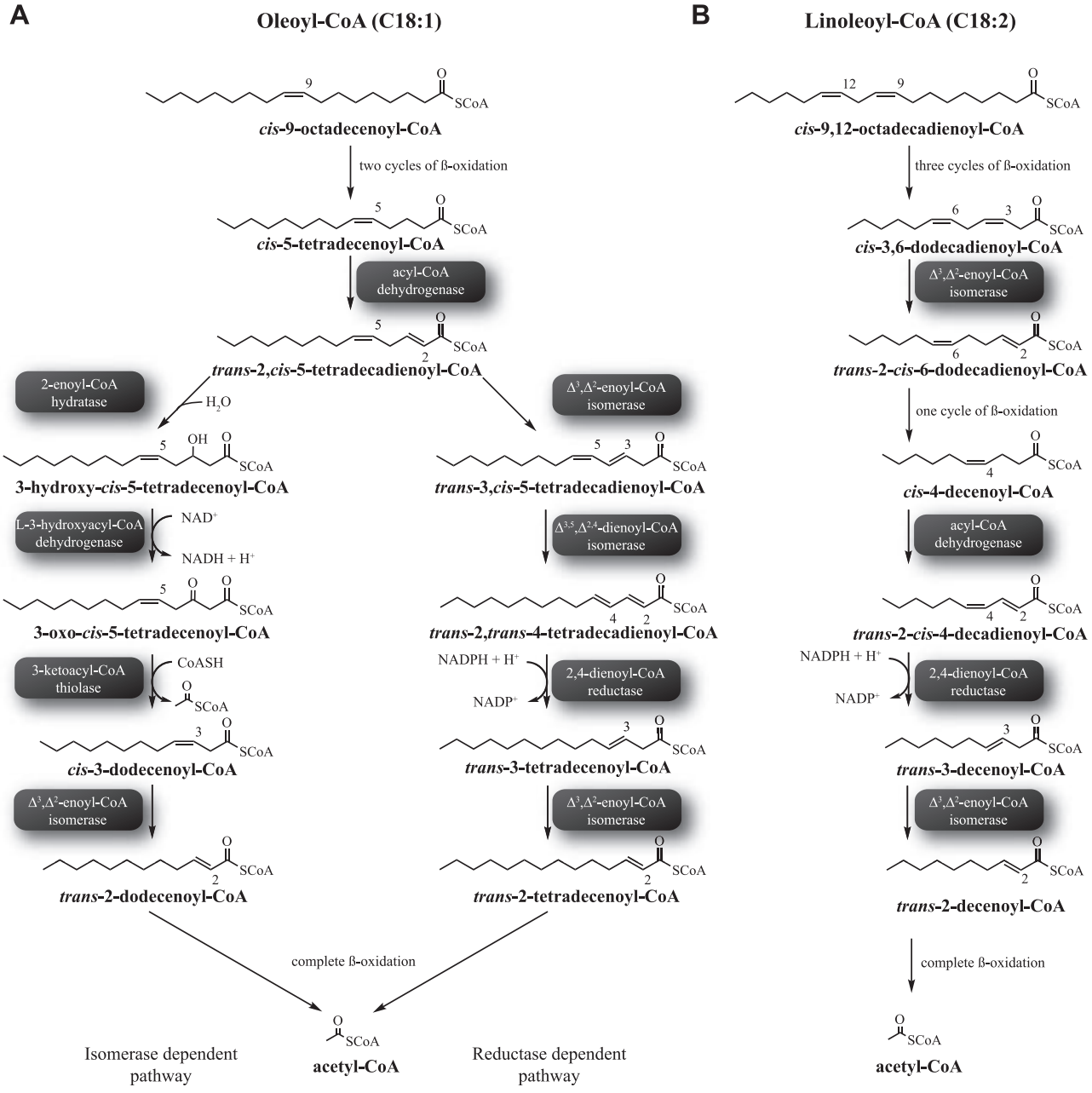

Figure 1. Mitochondrial β-oxidation of oleoyl-CoA and linoleoyl-CoA. *A*) The β-oxidation of oleoyl-CoA (C18:1-CoA) *via* the isomerase-dependent route and the reductase-dependent route. The major route for oleoyl-CoA oxidation is *via* the isomerase-dependent route (85%). Figure based on Ren *et al.* (3). *B*) The β-oxidation of linoleoyl-CoA (C18:2-CoA). Figure based on Schulz and Kunau (2).

the ECI belongs to the low similarity isomerase/hydratase superfamily of proteins (9,10). In mammalian cells, 3 proteins with ECI activity have been characterized, including the mitochondrial ECI localized exclusively in mitochondria (encoded by *Eci1*, formerly known as *Dci*; refs. 4–6), the peroxisomal ECI localized in mitochondria and peroxisomes (encoded by *Eci2*, formerly known as *Peci*; ref. 7), and EHHADH localized in peroxisomes (encoded by *Ehhadh*; ref. 8). Recently, we discovered a fourth ECI (*Eci3*), which is a mouse and rat specific protein (11). This ECI is expressed in peroxisomes of mouse kidney and is more ubiquitous in peroxisomes of rat tissue.

Although a human inherited metabolic disease has been described for most of the mitochondrial FAO enzymes, patients with ECI1 deficiency have yet to be identified. Such patients might have been missed because of unusual or mild phenotypes. To obtain more insight in the role of ECI1 in mitochondrial FAO, we further characterized a previously generated Eci1-deficient mouse model (12). This mouse model might be suitable to identify potential presentations of human ECI1 deficiency as well as to define diagnostic markers for ECI1 deficiency. It was reported that Eci1-deficient mice showed hepatic accumulation of lipids with unsaturated fatty acyl groups and developed dicarboxylic aciduria (12). We compared wild-type (WT) and Eci1-deficient mice fed a normal chow diet with mice that were denied access to food overnight or mice fed a diet containing a high content of unsaturated fatty acids. We found that Eci1-deficient mice have a tendency to develop hypoglycemia and are characterized by a unique and novel aberrant acylcarnitine profile. In addition, we show that the relatively mild phenotypic presentation of Eci1-deficient mice is caused by functional redundancy with Eci2.

MATERIALS AND METHODS

Materials

[U-^{13}C]-oleic acid (C18:1, *cis*-9) was purchased from Cambridge Isotope Laboratories (Andover, MA, USA); [U-^{13}C]-linoleic acid (C18:2, *cis*-9,12), myristoleic acid (C14:1, *cis*-9), dodecenoic acid (C12:1, *cis*-5), C12:0-CoA, and C14:0-CoA were purchased from Sigma-Aldrich (St. Louis, MO, USA). The 3-nonenoic acid was obtained from TCI Europe (Zwijndrecht, Belgium). The synthesis of 3-nonenoyl-CoA was performed as described by Rasmussen *et al.* (13). Purity of the product was determined by high-pressure liquid chromatography (HPLC) analysis. [9,10-^{3}H(N)]-palmitic acid and [9,10-^{3}H(N)]-oleic acid were purchased from PerkinElmer (Waltham, MA, USA) and bovine serum albumin (BSA; fatty acid free) from Sigma-Aldrich. The internal standards d_3-C0, d_3-C3, d_3-C6, d_3-C8, d_3-C10, and d_3-C16 carnitine were purchased from Dr. Herman J. ten Brink (Vrije Universiteit Medical Hospital, Amsterdam, The Netherlands).

Animal studies

Eci1-deficient mice on a mixed background were obtained from Memorec Biotec GmbH (Cologne, Germany; ref. 11). The colony was maintained by crossing with C57BL/6N (Charles River Breeding Laboratories, Inc., Wilmington, MA, USA). After 2 generations of backcrossing with C57BL/6, WT and Eci1-deficient mice were generated *via* heterozygous breeding pairs. Mice (WT, n=5; Eci1-deficient, n=7) were housed at 21 ± 1°C, 40–50% humidity, on a 12-h light-dark cycle, with *ad libitum* access to water and a standard rodent diet. At 6 wk of age, 50 μl of blood was collected from the vena saphena for the measurements of glucose, acylcarnitines, and ketones. At 7 wk of age, mice were weighed, placed in a clean cage without food but with access to water, and left overnight. This was followed by blood collection to obtain equivalent fasting blood level measurements. Immediately thereafter, mice were fed an olive oil-rich diet (diet 4021.82, 42% energy from fat; Arie Blok, Woerden, The Netherlands; for fatty acid composition see **Table 1**). Regular bleeding *via* the vena saphena was used for acylcarnitine measurements in blood. At 13 wk of age, mice were denied access to food for 24 h and anesthetized with an i.p. injection of 100 mg/kg pentobarbital. Anesthetized mice were euthanized by exsanguination from the vena cava inferior. The heart, liver, and muscles were rapidly excised, weighed, and processed for biochemical and histological analysis. All experiments were approved by the institutional review board for animal experiments at the Academic Medical Center (Amsterdam, The Netherlands).

Cell culture

Fibroblasts were obtained from WT and Eci1-deficient (mixed background) mouse ears and cultured in DMEM with glutamine, 10% fetal bovine serum (Gibco, Carlsbad, CA, USA), and 1% mixture of penicillin, streptomycin, fungizone (Gibco), and incubated in a CO_2 incubator (5% CO_2) at 37°C.

Antibodies and immunoblotting

The polyclonal antibodies against Eci1 and Eci2 were a generous gift from Dr. H. Schulz (Department of Chemistry, City College and Graduate School of the City University of New York, New York, NY, USA). The Eci2 antibody was affinity purified. Secondary antibodies goat anti-rabbit IrD cw800 were from Li-Cor Biosciences (Lincoln, NE, USA), and immunoblot images were obtained using the Odyssey infrared imaging system (Li-Cor Biosciences).

Acylcarnitine analysis

Fibroblasts cultured in 12-well plates were incubated for 72 h at 37°C, 5% CO_2 in MEM with 1% mixture of penicillin, streptomycin and Fungizone (Gibco) containing 0.4 mM L-carnitine, 0.4% BSA, and 100 μM of the indicated fatty acids. After 72 h, the incubation was stopped by removing the

TABLE 1. *Fatty acid content of the olive oil-rich diet*

Fatty acid	Percentage of total
C14:0	0.09
C16:0	10.46
C16:1ω9	0.58
C18:0	3.45
C18:1ω9	72.39
C18:1ω7	1.71
C18:1ω6	10.62
C18:3ω3	0.61
C20:0	0.10

medium from the cells, and cells were processed as described previously (14) using internal standards (50 pmol d_3-C3, 20 pmol d_3-C6, 20 pmol d_3-C8, 20 pmol d_3-C10, and 20 pmol d_3-C16 acylcarnitine). Semiquantitative determination of the formed acylcarnitines in the medium was performed using tandem mass spectrometry (15).

Plasma and blood acylcarnitines were measured as described previously (16) using internal standards (25 μM d_3-C0, 5 μM d_3-C3, 2 μM d_3-C6, 2 μM d_3-C8, 2 μM d_3-C10, and 2 μM d_3-C16 acylcarnitine).

FAO measurements

Palmitic and oleic acid oxidation were measured by quantifying the production of ^3H_2O from either [9,10-^{3}H(N)]-palmitic acid or [9,10-^{3}H(N)]-oleic acid as described previously by Manning *et al.* (17). The assay was performed in quadruplicate. The cells were incubated for 2 h at 37°C in Krebs-Henseleit buffer containing 0.1% (w/v) BSA, 100 μM palmitic or oleic acid, and a tracer of tritiated palmitic or oleic acid. Oxidation rate was expressed as nanomoles of fatty acid oxidized per hour per milligram of cell protein.

Clinical chemistry measurements

Glucose and β-hydroxybutyrate were measured in blood of WT and Eci1-deficient mice using standard enzymatic methods (18).

Quantitative real-time PCR

RNA was isolated from mouse tissue using Trizol extraction. cDNA was obtained by using the Superscript II Reverse Transcriptase Kit (Invitrogen, Carlsbad, CA, USA). Quantitative real-time PCR analysis of *Eci1*, *Eci2*, *Decr1*, *Cpt1a*, *Acadl*, *Ech1*, *Ehhadh*, *Ppargc1a*, and *Cyp4a10* were performed using the LC480 Sybr Green I Master mix (Roche Applied Science, Indianapolis, IN, USA). All samples were analyzed in duplicate. Data analysis was done using the linear regression as described by Ramakers *et al.* (19). For the comparison of the genes, the values were normalized against the housekeeping gene cyclophilin B. Primer sequences are available on request.

Synthesis of acylcarnitines standards

Commercially available C12:0-CoA and C14:0-CoA were used as substrates. The first step was the enzymatic conversion of C12:0-CoA or C14:0-CoA to *trans*-2-C12:1-CoA and *trans*-2-C14:1-CoA *via* acyl-CoA oxidase (from *Arthrobacter* sp.; Sigma-Aldrich; Reaction 1). For the second step, we used purified mitochondrial ECI (a gift of Dr. H. Schulz, City University of New York), which converted the formed *trans*-2-C12:1-CoA or *trans*-2-C14:1-CoA of Reaction 1 to either a *cis*-3-C12:1-CoA and *cis*-3-C14:1-CoA or a *trans*-3-C12:1-CoA and *trans*-3-C14:1-CoA (Reaction 2). The products of these reactions, as well as chemically synthesized *cis*-5 C12:1- and *cis*-5 C14:1-CoA, were then converted from a CoA ester to a carnitine ester by incubation with a homogenate of *S. cerevisiae* overexpressing CPT1a (Reaction 3; refs. 20, 21).

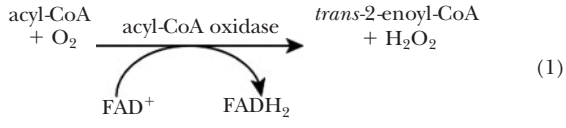

(1)

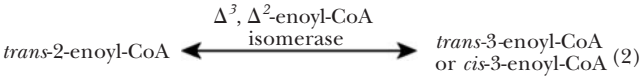

(2)

(3)

Acylcarnitine isomer measurements

An ultraperformance liquid chromatography (UPLC)–tandem mass spectrometry (MS/MS) system was used to analyze the acylcarnitine isomers. Samples were applied on a Waters Acquity BEH C18 column (100×2.1 mm, 1.7 μm; Waters Acquity, Milford, MA, USA). Separation of acylcarnitines was performed at a flow rate of 500 μl/min using gradient elution involving solvent A (0.1% heptafluorobutyric acid in water) and solvent B (100% methanol). Acylcarnitine esters were eluted using solvent B, increasing from 50 to 85% in 7 min, followed by a 2-min washing step with 100% solvent B and reequilibration of the column for 2 min with 100% solvent A in a total run time of 11 min. Acylcarnitine esters were detected using a Waters Quattro Premier XE MS/MS (Waters Acquity) set at the positive electrospray ionization (ESI) mode using nitrogen as nebulizing gas and argon as collision gas at a pressure of 2.5 e^{-3} mbar. Voltages were set at 3.5 kV capillary, 35 V cone, and 25 V collision energy. Acylcarnitine esters were measured using the following transitions: m/z 342.3 > 85.0 for C12:1 carnitine and m/z 370.3 > 85.0 for C14:1 carnitine. The system was operated by MassLynx 4.1 software (Waters Acquity).

Quantification of *cis*-3-C12:1 and *cis*-5-C14:1 acylcarnitine by HPLC-MS/MS

Quantification of *cis*-5-C14:1 acylcarnitine was performed using HPLC-MS/MS as described by Minkler *et al.* (22, 23). The *cis*-5-C14:1 acylcarnitine, d_3-*cis*-9-C14:1 acylcarnitine, and *trans*-2-C12:1 acylcarnitine were synthesized by small modifications to a standard method (24), purified by cation exchange SPE and preparative HPLC, and standardized by precisely determining their total carnitine content (22). Multiple-point calibration curves were constructed using d_3-*cis*-9-C14:1 acylcarnitine as the internal standard for *cis*-5-C14:1 and *trans*-2-C12:1 over 200-fold concentration ranges, ensuring accurate and precise absolute quantification of *cis*-5-C14:1 acylcarnitine. Quantification of *cis*-3-C12:1 acylcarnitine was performed using the calibration curve generated from *trans*-2-C12:1 and assuming that the responses of the two C12:1 acylcarnitines are identical.

Subcellular fractionation of mouse kidney

Subcellular fractionation of mouse kidney was performed as described previously (11). Kidney was obtained from WT and Eci1-deficient mice on a mixed background. Fractions of 1 ml were taken from the bottom of the gradient and were assayed for the marker enzymes glutamate dehydrogenase (GDH; mitochondria), catalase (peroxisomes), phosphoglucoisomerase (cytoplasm), β-hexosaminidase (lysosomes), and esterase (microsomes) as described previously (25, 26). Protein concentration was measured according to the method of Bradford (27), using BSA as standard.

ECI activity measurements

The ECI enzyme activity assay was performed by incubating protein samples for 5 min at 37°C in a medium containing: 100 mM TRIS buffer (pH 7.4) and 100 μM *trans*-3-nonenoyl-CoA in a final volume of 100 μl. The reaction was stopped by the addition of 10 μl 2M HCl and neutralized by adding 10 μl 2 M KOH/0.4 M MES. Acetonitrile (ACN) was added to the mixture

to a final concentration of 15% (v/v), followed by centrifugation for 5 min at 10,000 *g*. The reaction products were analyzed by reverse-phase HPLC using a Supelcosil LC-18-DB semiprep column (Supelco Analytical; Sigma-Aldrich). The column was developed isocratically using eluents containing 82% buffer A (10% ACN and 90% 16.9 mM $NaPO_4$, pH 6.9) and 18% buffer B (70% ACN and 30% 16.9 mM $NaPO_4$, pH 6.9) for 35 min at a flow rate of 3 ml/min followed by a wash step of 100% buffer B for 7 min at a flow rate of 3 ml/min. Absorbance of the eluate was continuously recorded using a spectrophotometer set at 260 nm. The substrate, *trans*-3-C9:1-CoA, yields one peak in the chromatogram. Incubation with purified isomerase yields two additional peaks in the chromatogram, the major product *trans*-2-C9:1-CoA, and a small peak, which we believe is *cis*-3-C9:1-CoA, which can be formed by the reverse reaction. In cell or tissue homogenates, the product *trans*-2-C9:1-CoA is further converted into L-3-hydroxy-C9:1-CoA as a result of the 2-enoyl-CoA hydratase (crotonase) activity. Therefore, we expressed ECI activity as the sum of the products formed by ECI and 2-enoyl-CoA hydratase, *i.e.*, *trans*-2-C9:1-CoA and L-3-hydroxy-C9:1-CoA.

Knockdown of Eci2 in mouse fibroblasts

For the production of virus containing shRNA against Eci2, HEK293 cells were transfected with pLKO.1-TRC cloning vector (Sigma-Aldrich), which contains a puromycin resistance cassette and a forward and a reverse annealed oligo (oligonucleotides used are mentioned below), psPAX2 (packaging plasmid for producing virus particles), and pMD2.G (envelope plasmid for producing virus particles; Sigma-Aldrich) using Lipofectamine 2000 (Invitrogen) according to the manufacturer's protocol. Cells were grown overnight, and medium containing the virus with shRNA1, shRNA2, or shRNA3 was collected. WT and Eci1-deficient fibroblasts were exposed to the medium containing the shRNA and were selected by adding 5 μg/ml puromycin. Oligonucleotides used for the knockdown of Eci2: shRNA1 primer *Mus musculus* (*Mm*), fw pECI 5′-CCGGAAGCTAAGACTCTATG-CACTGCTCGAGCAGTGCATAGAGTCTTAGCTTTTTTTG-3′, rev 5′-AATTCAAAAAAAGCTAAGACTCTATGCACTGCTCGAG-CAGTGCATAGAGTCTTAGCTT-3′; shRNA2 primer *Mm* pECI, fw 5′-CCGGAAGACATCCTGGTAACTTCTGCTCGAGCAGAAGT-TACCAGGATGTCTTTTTTTG-3′, rev 5′-AATTCAAAAAAAGA-CATCCTGGTAACTTCTGCTCGAGCAGAAGTTACCAGGAT-GTCTT-3′; shRNA3 primer *Mm* pECI, fw 5′-CCGGA-AGCCTCTGGTTGCGGTAGTACTCGAGTACTACCGCAACCA-GAGGCTTTTTTTG-3′, rev 5′-AATTCAAAAAAAGCCTCTGGTT-GCGGTAGTACTCGAGTACTACCGCAACCAGAGGCTT-3′. All three sets led to knockdown of Eci2 and identical biochemical changes. The results for oligo set 3 are shown, as the knockdown was slightly more efficient for these oligonucleotides.

Statistics

Statistical analysis was performed using GraphPad Prism 5 (GraphPad, La Jolla, CA, USA). Data are presented as means ± SD. Differences were evaluated using a 2-sided *t* test or a 1-way analysis of variance (ANOVA) with Bonferroni's multiple comparison test. Statistical significance is indicated as follows: $*P < 0.05$, $**P < 0.01$ and $***P < 0.001$.

RESULTS

Mild phenotypic presentation of Eci1-deficient mice

Janssen and Stoffel (12) established that upon food withdrawal, Eci1-deficient mice accumulate lipids with unsaturated fatty acyl groups in the liver and develop dicarboxylic aciduria. Other characteristic derangements observed in inherited FAO defects, such as an aberrant acylcarnitine profile or hypoketotic hypoglycemia were not reported. Initially, we studied WT and Eci1-deficient mouse fibroblasts and determined the effect of Eci1 deficiency on FAO in these fibroblasts. We compared the oxidation rate of oleic acid to palmitic acid and surprisingly found no difference (**Table 2**). This indicates that *in vitro* in fibroblasts, oxidation of unsaturated fatty acids is only minimally affected by Eci1 deficiency. To characterize the effect of Eci1 deficiency on the metabolism of unsaturated fatty acids *in vivo*, we compared WT and Eci1-deficient mice fed a normal chow diet in the fed state and after overnight food withdrawal. Upon food withdrawal, Eci1-deficient mice showed a trend to lower blood glucose levels when compared to WT mice ($P=0.09$; **Fig. 2*B***). Ketone body (*i.e.*, β-hydroxybutyrate) levels in the fed state and after overnight withdrawal of food ("fasted" state) were not different between Eci1-deficient and WT mice (Fig. 2*B*). Next, we determined the acylcarnitine profile in blood, plasma, liver, and heart of WT and Eci1-deficient mice. MS/MS analysis of the acylcarnitines in body fluids and tissue is the gold standard for the clinical diagnostics of FAO disorders. In the fed condition, Eci1-deficient mice showed a slight accumulation of C10:1, C12:1, and C14:1 acylcarnitines in blood (Fig. 2*C*) and plasma (data not shown). After overnight food withdrawal, Eci1-deficient mice displayed an increase in the accumulation of unsaturated acylcarnitines. In blood, we detected the accumulation of C10:1, C12:2, C12:1, C14:2, C14:1, and C16:2 acylcarnitines (Fig. 2*C*). In liver and heart, a slight increase in C12:1 and C14:1 acylcarnitines was observed (Fig. 2*D*). Thus, Eci1-deficient mice are characterized by a tendency to develop ketotic hypoglycemia and a unique and novel aberrant acylcarnitine profile.

Olive oil-rich diet increases unsaturated acylcarnitine accumulation in Eci1-deficient mice

To further define the effect of Eci1 deficiency on the oxidation of unsaturated fatty acids, WT and Eci1-deficient mice were fed an olive oil-rich diet containing 42% of energy derived from fat (for fatty acid composition see Table 1). Biochemical parameters in blood were measured at several consecutive time points during this feeding regimen. Eci1-deficient mice fed an olive oil-rich diet displayed an increase in the accumulation of C12:1 and C14:1 acylcarnitines when compared with mice fed a normal chow diet (Fig. 2*E*),

TABLE 2. β-*Oxidation of oleic and palmitic acid*

Genotype	Oleic acid ($nmol \cdot mg^{-1} \cdot h^{-1}$)	Palmitic acid ($nmol \cdot mg^{-1} \cdot h^{-1}$)	Oleic/palmitic ratio
WT	17.9	17.6	1.02
WT	10.6	12.9	0.82
Eci1 KO	13.8	14.7	0.94
Eci1 KO	12.3	12.4	0.99

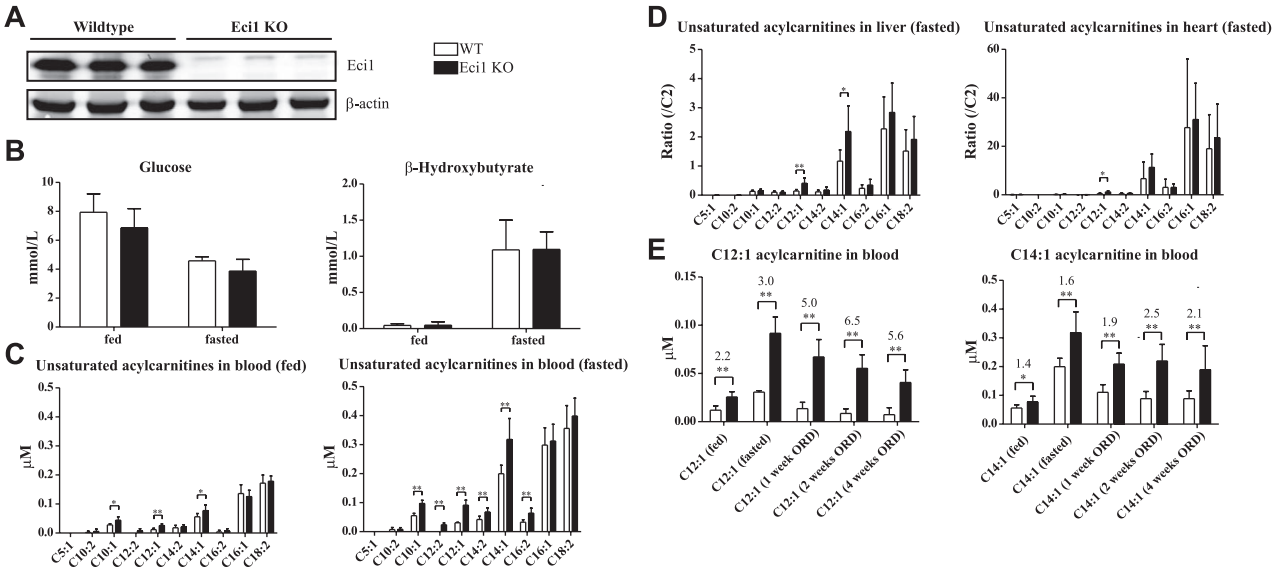

Figure 2. Metabolite levels in blood, plasma, liver and heart of WT and Eci1-deficient mice. *A*) Immunoblot analysis of Eci1 in WT and Eci1-deficient mouse hearts showing the absence of Eci1 in the Eci1-deficient mice. *B*) Glucose levels (mM) in blood of overnight "fasted" (denied access to food) WT and Eci1-deficient mice fed a chow diet. Blood β-hydroxybutyrate levels in WT and Eci1-deficient mice fed a chow diet in the fed and fasted state (mM). *C*) Acylcarnitine profiles in blood of WT and Eci1-deficient mice fed a chow diet in the fed and overnight fasted state (in μM). *D*) Acylcarnitine profiles in liver and heart of WT and Eci1-deficient mice fed a chow diet in fasted state. Ratio of the acylcarnitines with acetylcarnitine is displayed. *E*) Levels of C12:1 and C14:1 acylcarnitine measured in blood of WT and Eci1-deficient mice in the fed and fasted state when fed a chow diet and in the fed state when fed an olive oil-rich diet (ORD) for different duration as indicated. Numbers indicate fold increase. Error bars = SD. $^*P < 0.05$, $^{**}P < 0.01$.

demonstrating that Eci1 plays a role in the oxidation of oleic acid. In time, the absolute acylcarnitine levels decreased; however, the fold change with WT mice remained similar (Fig. 2*E*). This suggests compensatory adaptation to the olive oil-rich diet in WT and Eci1-deficient mice.

cis-3-C12:1 and *cis*-5-C14:1 acylcarnitine accumulate in Eci1-deficient mice

The acylcarnitine profile of mice denied access to food overnight and mice fed an olive oil-rich diet showed an increase in the accumulation of C12:1 and C14:1 acylcarnitine in blood and liver (Fig. 2*C–E*). Taking the isomerase- and the reductase-dependent route into account (3), we hypothesized that the isomers accumulating were the *cis*-3-C12:1 and the *trans*-3-C14:1 acylcarnitines (Fig. 1). To identify the different isomers of C12:1 and C14:1 acylcarnitine, we used chemically and enzymatically prepared isomers of C12:1 and C14:1 acylcarnitine and analyzed them by UPLC-MS/MS. Using this approach, we were able to discriminate between the *cis*-5, *cis*-3, *trans*-3, and *trans*-2 isomers of C12:1 acylcarnitine, and the *cis*-9, *cis*-5, *cis*-3, *trans*-3 and *trans*-2 isomers of C14:1 acylcarnitine (**Fig. 3*A***). In the blood of Eci1-deficient mice, we detected 4 peaks for C12:1 acylcarnitine, identified as *cis*-5-C12:1 acylcarnitine (peak 2), *cis*-3-C12:1 acylcarnitine (peak 3), and *trans*-3-C12:1 acylcarnitine (peak 4; Fig. 3*A*, top panel). The fourth peak (marked by a question mark in Fig. 3*A*) may be *cis*-9 or *cis*-7-C12:1 acylcarnitine. As expected, and consistent with the isomerase-dependent pathway, *cis*-3 C12:1 acylcarnitine was the most abundant isomer.

For C14:1 acylcarnitine, 2 peaks were identified: *cis*-9-C14:1 acylcarnitine (peak 1) and *cis*-5-C14:1 acylcarnitine (peak 2). This accumulation of *cis*-5-C14:1 acylcarnitine is unexpected and not consistent with the reductase-dependent pathway. We have previously identified *cis*-5-C14:1 acylcarnitine as the primary accumulating acylcarnitine in the LCAD-knockout (KO) mice (14). The accumulation of *cis*-5-C14:1 acylcarnitine in Eci1-deficient mice was confirmed by a direct comparison with blood from LCAD-KO mice (Fig. 3*A*). Thus, accumulation of *cis*-5-C14:1 acylcarnitine is consistent with inhibition at the level of LCAD.

In addition, we accurately quantified *cis*-3-C12:1 (assumed to have the same response as the standard *trans*-2-C12:1) and *cis*-5-C14:1 acylcarnitine (for which we have standardized calibrants). Both acylcarnitines were significantly increased in the blood of Eci1-deficient mice (Fig. 3*B* and Supplemental Fig. S1). These data suggest that the breakdown of *cis*-9-C18:1 occurs primarily *via* the isomerase-dependent pathway. The accumulation of *cis*-5-C14:1 indicates that in Eci1-deficient mice, FAO is inhibited also at the level of LCAD. We found no metabolites indicative of the reductase-dependent pathway.

Absence of compensatory up-regulation of other ECIs in Eci1-deficient mice

Given the mild phenotypic presentation of Eci1 deficiency in mice, we performed expression analysis to identify potential compensatory mechanisms, with a special focus on the other ECIs and the peroxisome proliferator-activated receptor α (PPARα) signaling pathway. Expression levels of PGC1α (*Ppargc1a*), Eci2, Ech1, Cpt1a, Cyp4a10, and Decr1 were similar in livers of fasted-state WT and Eci1-deficient mice (**Fig. 4**). There was a small increase in the expression of Acadl, Pdk4, and Ehhadh in

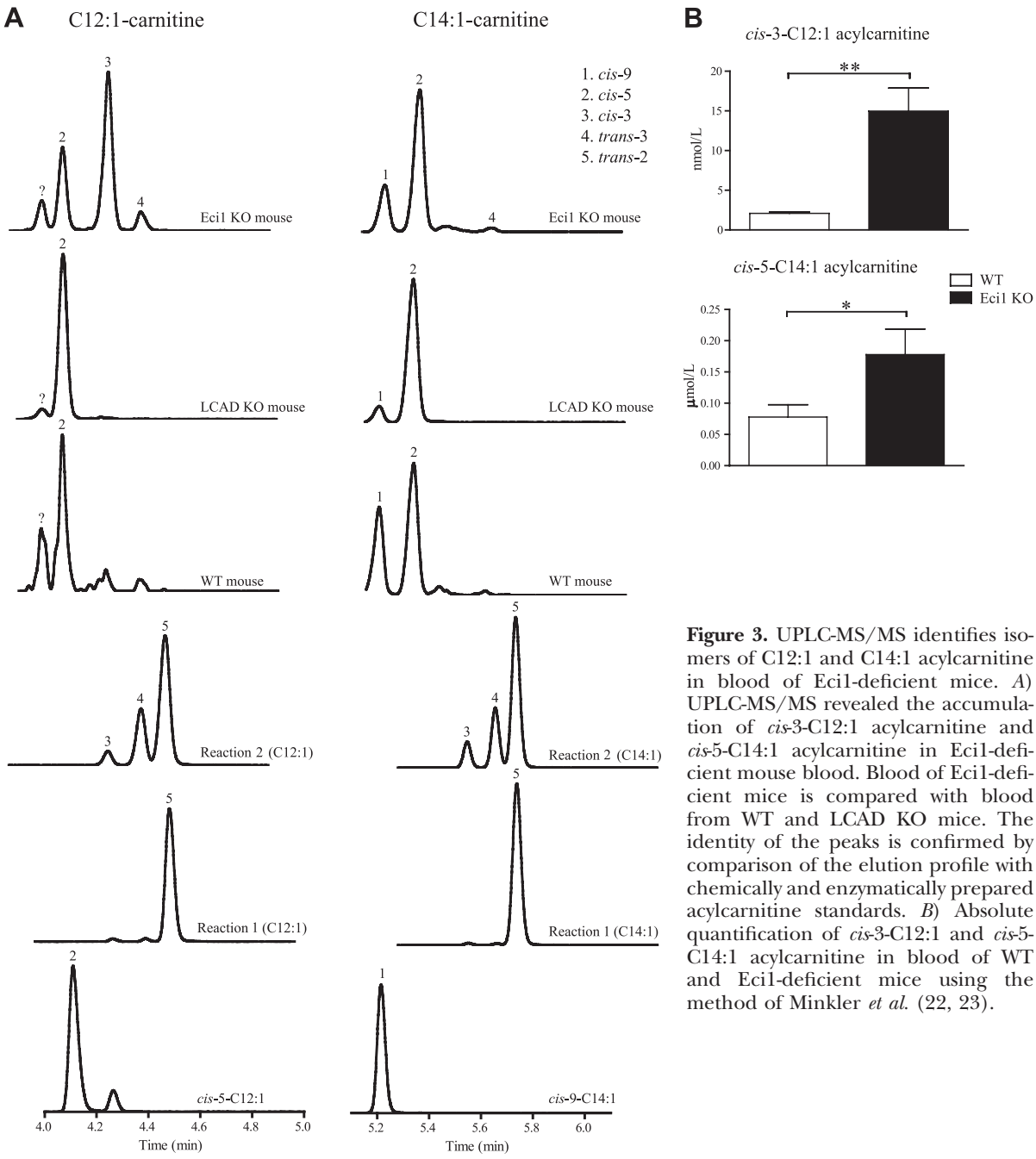

Figure 3. UPLC-MS/MS identifies isomers of C12:1 and C14:1 acylcarnitine in blood of Eci1-deficient mice. *A*) UPLC-MS/MS revealed the accumulation of *cis*-3-C12:1 acylcarnitine and *cis*-5-C14:1 acylcarnitine in Eci1-deficient mouse blood. Blood of Eci1-deficient mice is compared with blood from WT and LCAD KO mice. The identity of the peaks is confirmed by comparison of the elution profile with chemically and enzymatically prepared acylcarnitine standards. *B*) Absolute quantification of *cis*-3-C12:1 and *cis*-5-C14:1 acylcarnitine in blood of WT and Eci1-deficient mice using the method of Minkler *et al.* (22, 23).

the Eci1-deficient mouse liver, suggesting that the PPARα pathway was more active (Fig. 4). Janssen and Stoffel (12) also observed an increase of selected PPARα target genes after 24 and 48 h of food withdrawal, which supports our finding. Despite this finding, these data show that the mild phenotypic presentation of Eci1-deficient mice is not due to activation of compensatory pathways, as the expression of none of the other ECIs was up-regulated at the transcriptional level. This suggests that similar expression levels of other ECIs are sufficient to compensate for Eci1 deficiency.

Residual ECI activity in mitochondria of Eci1-deficient mice

It is known that Eci2, formerly known as the peroxisomal ECI, is also localized to the mitochondria (28). To prove that mitochondria harbor more than one ECI, we performed subcellular fractionation of WT and Eci1-deficient mouse kidney and measured the ECI activity in the different fractions. In WT kidney, we detected ECI activity in the mitochondrial fraction. In the mitochondrial fraction of Eci1-deficient mouse kidney; however, there was still substantial residual ECI activity (**Fig. 5**). Therefore, we conclude that there is additional ECI activity in the mitochondria of Eci1-deficient mice.

Eci2 is responsible for the residual ECI activity in Eci1-deficient fibroblasts

To prove that Eci2 is responsible for the residual ECI activity in the mitochondria of Eci1-deficient mice, we knocked down Eci2 expression in Eci1-deficient fibro-

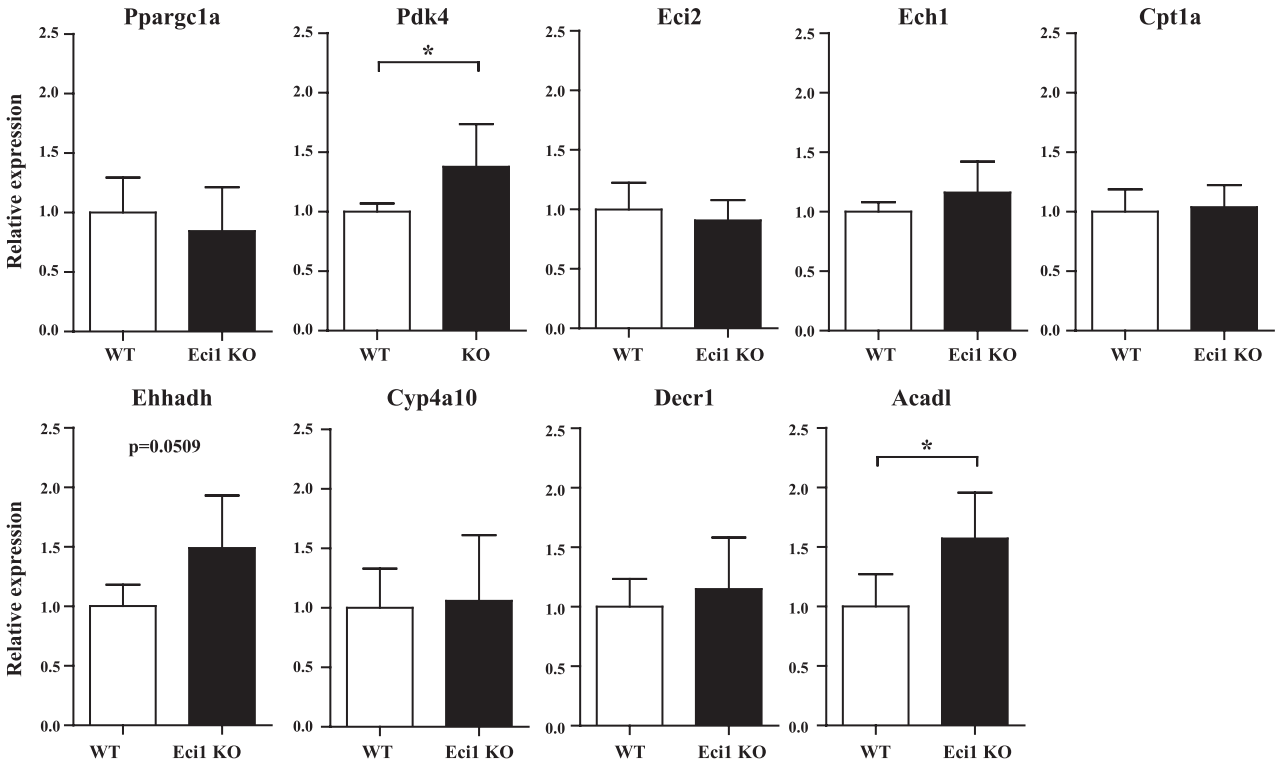

Figure 4. mRNA expression levels in fasted-state WT and Eci1-deficient mouse livers. Relative expression levels of PGC1α (*Ppargc1a*), Eci2, Ech1, Cpt1a, Ehhadh, Cyp4a10, Decr1, Acadl, and Pdk4 in mouse liver. Expression is corrected for cyclophilin B. Error bars = SD. $*P < 0.05$.

blasts. Eci2 protein levels were decreased by 90% in WT and Eci1-deficient fibroblasts, as shown by Western blot analysis (**Fig. 6*A***). Furthermore, we measured ECI activity in these fibroblasts (Fig. 6*B*). Considerable residual ECI activity was detected in the Eci1-deficient fibroblasts and the WT fibroblasts with a knockdown for Eci2. The most deficient ECI activity was observed in the Eci1-deficient fibroblast, in which Eci2 was knocked down. This small residual ECI activity in the Eci1-deficient fibroblasts with a knockdown for Eci2 may be due to EHHADH, which is localized in the peroxisomes of these fibroblasts, or incomplete Eci2 knockdown. To determine the effect of combined Eci1 and Eci2 deficiency on FAO in these fibroblasts, we incubated the fibroblasts with [U-^{13}C]-oleic or [U-^{13}C]-linoleic acid (Fig. 6*C*). The formation of acylcarnitines was measured in the culture medium. On incubation with oleic acid, the Eci1-deficient fibroblasts have slightly elevated levels of C12:1 and C14:1 acylcarnitines, which became more pronounced after the knockdown of Eci2 (Fig. 6*C*). Furthermore, in these fibroblasts, the *cis*-3-C12:1 and *cis*-5-C14:1 isomers were responsible for the accumulation of C12:1 and C14:1 acylcarnitines, consistent with the results obtained in the blood of the Eci1-deficient mice (Supplemental Fig. S1). Knockdown of Eci2 in WT fibroblasts does not lead to a significant increase in acylcarnitines on oleic acid incubation. On incubation with linoleic acid, Eci1-deficient fibroblasts have slightly elevated levels of C10:1, C12:2, C14:2, and C18:2 acylcarnitines. Combined Eci1 and Eci2 deficiency prominently increases C12:2 accumulation and also leads to a further increase of C10:1, C14:2, and C18:2 acylcarnitines (Fig. 6*C*). Knockdown of Eci2 in WT fibroblasts

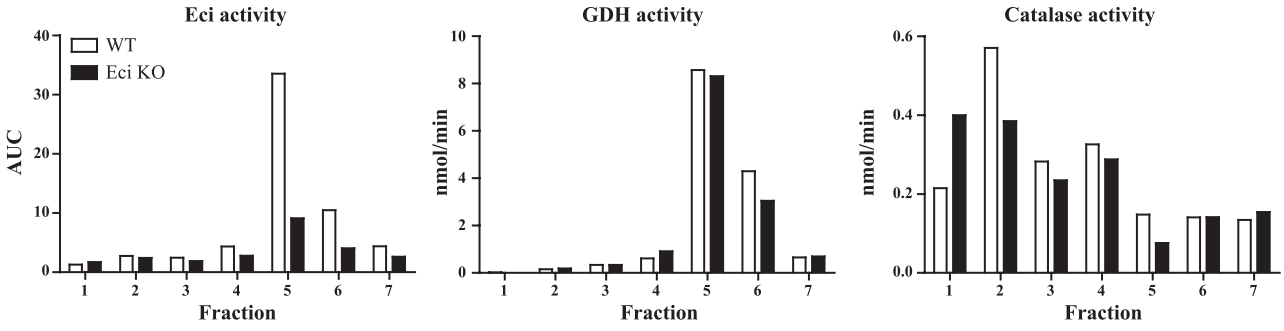

Figure 5. Subcellular fractionation of ECI activity in kidney. Subcellular fractionation of WT and Eci1-deficient mouse kidney revealed residual isomerase activity in the mitochondria of the Eci1-deficient mice. GDH and catalase activity were measured as marker enzymes for fractions containing mitochondrial or peroxisomal proteins, respectively (in nmol/min).

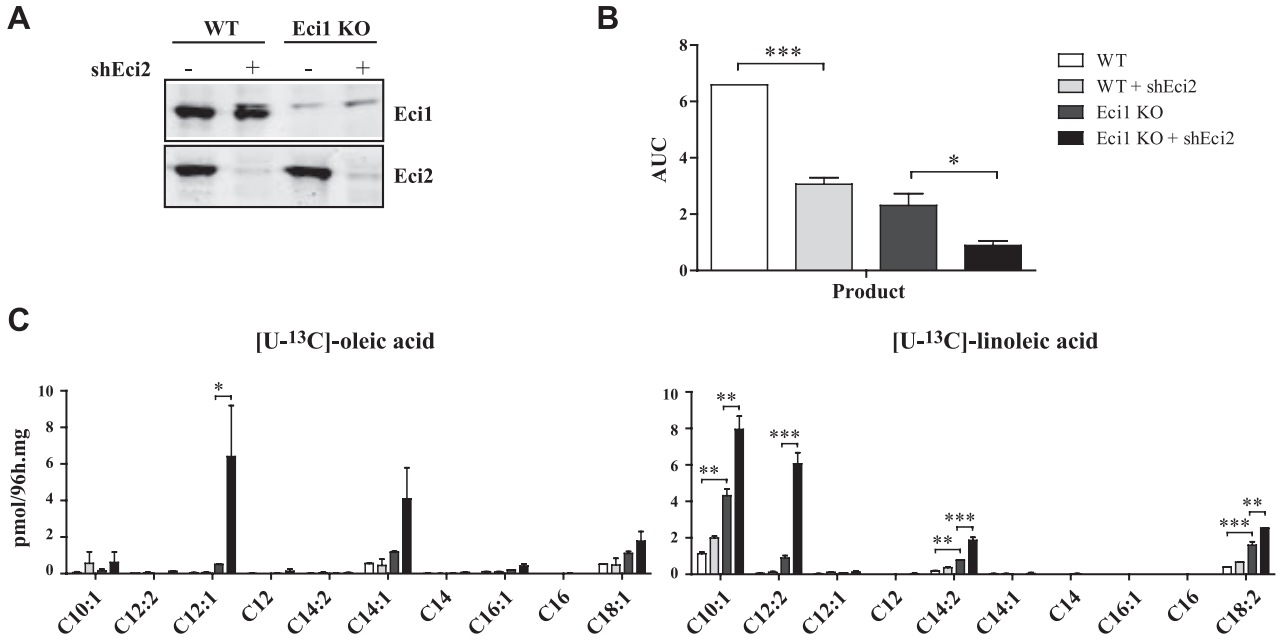

Figure 6. Eci2 is responsible for the residual ECI activity in the mitochondria of Eci1-deficient mice. *A*) Western blot analysis using antibodies against Eci1 and Eci2 revealed a knockdown for Eci2 of 90% in the WT and Eci1-deficient mouse fibroblasts. *B*) ECI activity measurements in WT and Eci1-deficients fibroblast with or without Eci2 knockdown. *C*) Acylcarnitine profile in medium of WT and Eci1-deficient fibroblasts with or without Eci2 knockdown incubated with [U-^{13}C]-oleic or [U-^{13}C]-linoleic acid. Error bars = SD. $*P < 0.05$, $**P < 0.01$, $***P < 0.001$.

does not lead to a significant increase in acylcarnitines on linoleic acid incubation. From these data we conclude that Eci2 is responsible for the residual ECI activity in mitochondria of Eci1-deficient mice.

DISCUSSION

Several mouse models for FAO disorders have been generated and characterized. Mice deficient in one of the enzymes of FAO may present with a similar phenotype as human patients. For example, the LCAD-KO mice serve as a model for human very long chain acyl-CoA dehydrogenase (VLCAD) deficiency because these mice display hypoketotic hypoglycemia and accumulation of specific acylcarnitines, as well as cardiac hypertrophy (14, 29–31). Although a human inherited metabolic disease has been described for most of the mitochondrial FAO enzymes, patients with a deficiency in one of the ECIs have yet to be identified. These patients might have been missed because of unusual or mild phenotypes. To obtain more insight in the role of ECI1 in mitochondrial FAO, we further characterized a previously generated Eci1-deficient mouse model (12). This mouse model might be suitable to identify potential presentations of human ECI1 deficiency as well as to define diagnostic markers for ECI1 deficiency. We focused on the acylcarnitine accumulation, as this currently constitutes the main tool in the diagnostics of FAO disorders.

Initially, we used Eci1-deficient mouse fibroblasts. In these fibroblasts, the rate of oleic acid and palmitic acid oxidation was not different when compared to WT fibroblasts, indicating a mild metabolic defect. Next, we studied Eci1-deficient mice. Overnight food withdrawal or feeding an olive oil-rich diet caused accumulation of C12:1 and C14:1 acylcarnitines in blood and tissues of Eci1-defcient mice. Moreover, Eci1-deficient mice display mild food withdrawal-induced ketotic hypoglycemia. Interestingly, Decr1-deficient mice, in which another auxiliary FAO enzyme is defective, also have ketotic hypoglycemia, albeit more severe (32). This suggests that defects in different auxiliary enzymes are characterized by ketotic hypoglycemia. Similar to humans, mouse models for FAO defects, such as Decr1- and LCAD-deficient mice, have a prominent fatty liver (14,32). In contrast to the initial observation by Janssen and Stoffel (12), Eci1-deficient mice do not have hepatic steatosis. This might be caused by a difference in the duration of the food-withdrawal period; Janssen and Stoffel analyzed after 48h of food withdrawal, while we performed an overnight food withdrawal. Cardiac hypertrophy, which is present in LCAD-deficient mice (29), was absent in both Eci1-and Decr1-deficient mice ((32) and data not shown). Thus, overall, the phenotypic presentation of Eci1 deficiency in mice is relatively mild.

By using UPLC-MS/MS, we found that *cis*-3-C12:1 and *cis*-5-C14:1 acylcarnitine accumulate, and not *trans*-3-C14:1 acylcarnitine. Accumulation of *trans*-3-C14:1 acylcarnitine was expected if the oleic acid would be oxidized *via* the reductase-dependent pathway (Fig. 1*A*). Therefore, we conclude that the breakdown of oleic acid is primarily proceeding *via* the isomerase-dependent pathway, as was originally proposed by Ren and Schulz (3), which is in line with the accumulation of *cis*-3-C12:1 acylcarnitine. In the murine FAO pathway, the *cis*-5-C14:1-CoA is known to be the substrate for LCAD, concluded from the fact that its acylcarnitine ester, *cis*-5-C14:1 acylcarnitine, is the primary metabolite accumulating in the LCAD-KO mice

(14). We speculate that the accumulation of the primary substrate for Eci1 (*cis*-3-C12:1-CoA) inhibits the enzyme activity of LCAD, resulting in elevated levels of *cis*-5-C14:1-CoA and as a consequence *cis*-5-C14:1 acylcarnitine. In humans, expression of LCAD is very low, and VLCAD is the major enzyme involved in metabolism of *cis*-5-C14:1-CoA, therefore a potential human ECI1 deficiency may not present with C14:1 acylcarnitine accumulation.

In peroxisomes, Eci2 is the major monofunctional isomerase; however, Eci2 also is known to be localized in the mitochondria (28). Eci1 deficiency in mice leads to a mild phenotype, suggesting that Eci2 can compensate for Eci1 deficiency in mitochondria. It is important to realize that this compensation can occur without an increase in the expression levels of Eci2 (Fig. 4). Indeed, when we knocked down Eci2 in the Eci1-deficient mouse fibroblasts, more pronounced accumulation of the unsaturated acylcarnitines was observed when incubated with either oleic acid or linoleic acid. When Eci2 was knocked down in WT mouse fibroblasts, no accumulation of unsaturated fatty acids was observed. This further substantiates that both ECIs can compensate for each other's deficiency and thus are, at least in part, functionally redundant in unsaturated FAO.

Despite this functional redundancy, our data prove that both Eci1 and Eci2 play a role in the oxidation of oleic acid, with Eci1 being slightly more important. In addition, we also prove that Eci1 and Eci2 are involved in the oxidation of linoleic acid, again with a high degree of functional redundancy. Based on the pathway proposed by Schulz and Kunau (2), ECI activity is crucial for the conversion of two metabolites in linoleic acid degradation (Fig. 1*B*; *cis*-3,*cis*-6-C12:2-CoA, and *trans*-3-C10:1-CoA). Indeed, on incubation with [U-^{13}C]-linoleic acid, we observed accumulation of labeled C10:1 and C12:2 acylcarnitine. Therefore, we speculate that these acylcarnitines are the *cis*-3,*cis*-6-C12:2 acylcarnitine and the *trans*-3-C10:1 acylcarnitine. Since standards for these specific isomers are not yet available, we could not confirm the identity of these acylcarnitines.

The questions that remain are why there are two ECIs present in the mitochondria, and why there are no unsaturated acylcarnitines accumulating in WT fibroblasts in which Eci2 has been knocked down. A previous study, in which the substrate specificity of the mitochondrial ECIs was characterized, provided evidence that Eci1 is the dominant enzyme in catalyzing the conversions of *cis*-3-enoyl-CoA to *trans*-2-enoyl-CoA and *trans*-2,*cis*-5-enoyl-CoA to *trans*-3,*cis*-5-enoyl-CoA, whereas Eci2 contributes significantly to the conversion of *trans*-3-enoyl-CoA to *trans*-2-enoyl-CoA (28). This is in line with our data and suggests that the oxidation of oleic and linoleic acid is more dependent on the isomerase-dependent pathway, with Eci1 as the most important isomerase. Eci2 could be more important for the oxidation of *trans* fatty acids such as elaidic acid (*trans*-9-C18:1). As *trans* fatty acids are only present in small amounts in rodent chow and our diet, they do not contribute to the observed acylcarnitine profiles. Furthermore, we cannot exclude that EHHADH (located in peroxisomes) could partially compensate for Eci1 and Eci2 deficiency as well. This, however, seems unlikely, as EHHADH is predicted to be involved in catalyzing the reaction of *trans*-2,*cis*-5-enoyl-CoA to *trans*-3,*cis*-5-enoyl-CoA (28).

In summary, in mice a deficiency of Eci1 leads to a mild metabolic phenotypic presentation due to a high degree of functional redundancy of Eci1 and Eci2. Therefore, human ECI1 deficiency might have been missed because of a very mild presentation or no disease presentation at all. Based on our studies, we suggest screening patients with a mild ketotic hypoglycemia for an accumulation of C10:1, C12:2, and C12:1 acylcarnitines, which are specific for Eci1-deficiency in mice. This might lead to future identification of ECI1-deficient patients. FJ

The authors thank Dr. H. Schulz (Department of Chemistry, City College and Graduate School of the City University of New York, New York, NY, USA) for the generous gift of the polyclonal mouse Eci1 and Eci2 antibody, Dr. C. Argmann for critically reading the manuscript, W. Smit for the analysis of the fatty acid composition of the diet, and the employees of the Animal Research Institute (Amsterdam, The Netherlands) for technical assistance. This work was supported by the Netherlands Organization for Scientific Research (VIDI; grant 016.086.336 to S.M.H.) and the Ter Meulen Fund, Royal Netherlands Academy of Arts and Sciences, The Netherlands (to M.V.W.).

REFERENCES

1. Hiltunen, J. K., and Qin, Y. (2000) beta-oxidation - strategies for the metabolism of a wide variety of acyl-CoA esters. *Biochim. Biophys. Acta.* **1484,** 117–128
2. Schulz, H., and Kunau, W. H. (1987) Beta-oxidation of unsaturated fatty acids - A revised pathway. *Trends Biochem. Sci.* **12,** 403–406
3. Ren, Y., and Schulz, H. (2003) Metabolic functions of the two pathways of oleate beta -oxidation double bond metabolism during the beta -oxidation of oleic acid in rat heart mitochondria. *J. Biol. Chem.* **278,** 111–116
4. Stoffel, W., Ditzer, R., and Caesar, H. (1964) [The metabolism of unsaturated fatty acid. 3. On the beta-oxidation of mono- and polyene-fatty acids. The mechanism of the enzymatic reaction on delta-3-cis-enoyl-CoA compounds]. *Hoppe Seylers Z. Physiol. Chem.* **339,** 167–181
5. Palosaari, P. M., Kilponen, J. M., Sormunen, R. T., Hassinen, I. E., and Hiltunen, J. K. (1990) Delta 3,delta 2-enoyl-CoA isomerases. Characterization of the mitochondrial isoenzyme in the rat. *J. Biol. Chem.* **265,** 3347–3353
6. Müller-Newen, G., and Stoffel, W. (1991) Mitochondrial 3-2trans-Enoyl-CoA isomerase. Purification, cloning, expression, and mitochondrial import of the key enzyme of unsaturated fatty acid beta-oxidation. *Biol. Chem. Hoppe Seyler* **372,** 613–624
7. Geisbrecht, B. V., Zhang, D., Schulz, H., and Gould, S. J. (1999) Characterization of PECI, a novel monofunctional Delta(3), Delta(2)-enoyl-CoA isomerase of mammalian peroxisomes. *J. Biol. Chem.* **274,** 21797–21803
8. Palosaari, P. M., and Hiltunen, J. K. (1990) Peroxisomal bifunctional protein from rat liver is a trifunctional enzyme possessing 2-enoyl-CoA hydratase, 3-hydroxyacyl-CoA dehydrogenase, and delta 3, delta 2-enoyl-CoA isomerase activities. *J. Biol. Chem.* **265,** 2446–2449
9. Müller-Newen, G., Janssen, U., and Stoffel, W. (1995) Enoyl-CoA Hydratase and Isomerase form a superfamily with a common active-site glutamate residue. *European. J. Biochem.* **228,** 68–73
10. Palosaari, P. M., Vihinen, M., Mantsala, P. I., Alexson, S. E., Pihlajaniemi, T., and Hiltunen, J. K. (1991) Amino acid sequence similarities of the mitochondrial short chain delta 3, delta 2-enoyl-CoA isomerase and peroxisomal multifunctional delta 3, delta 2-enoyl-CoA isomerase, 2-enoyl-CoA hydratase, 3-hydroxyacyl-CoA dehydrogenase enzyme in rat liver. The

proposed occurrence of isomerization and hydration in the same catalytic domain of the multifunctional enzyme. *J. Biol. Chem.* **266,** 10750–10753
11. Ofman, R., Speijer, D., Leen, R., and Wanders, R. J. (2006) Proteomic analysis of mouse kidney peroxisomes: identification of RP2p as a peroxisomal nudix hydrolase with acyl-CoA diphosphatase activity. *Biochem. J.* **393,** 537–543
12. Janssen, U., and Stoffel, W. (2002) Disruption of mitochondrial beta -oxidation of unsaturated fatty acids in the 3,2-trans-enoyl-CoA isomerase-deficient mouse. *J. Biol. Chem.* **277,** 19579–19584
13. Rasmussen, J. T., Borchers, T., and Knudsen, J. (1990) Comparison of the binding affinities of acyl-CoA-binding protein and fatty-acid-binding protein for long-chain acyl-CoA esters. *Biochem. J.* **265,** 849–855
14. Chegary, M., te Brinke, H., Ruiter, J. P., Wijburg, F. A., Stoll, M. S., Minkler, P. E., van Weeghel, M., Schulz, H., Hoppel, C. L., Wanders, R. J., and Houten, S. M. (2009) Mitochondrial long chain fatty acid beta-oxidation in man and mouse. *Biochim. Biophys. Acta* **1791,** 806–815
15. Ventura, F. V., Costa, C. G., Struys, E. A., Ruiter, J., Allers, P., Ijlst, L., Tavares de Almeida, I., Duran, M., Jakobs, C., and Wanders, R. J. (1999) Quantitative acylcarnitine profiling in fibroblasts using [U-13C] palmitic acid: an improved tool for the diagnosis of fatty acid oxidation defects. *Clin. Chim. Acta* **281,** 1–17
16. Vreken, P., van Lint, A. E., Bootsma, A. H., Overmars, H., Wanders, R. J., and van Gennip, A. H. (1999) Quantitative plasma acylcarnitine analysis using electrospray tandem mass spectrometry for the diagnosis of organic acidaemias and fatty acid oxidation defects. *J. Inherit. Metab. Dis.* **22,** 302–306
17. Manning, N. J., Olpin, S. E., Pollitt, R. J., and Webley, J. (1990) A comparison of [9,10-3H]palmitic and [9,10-3H]myristic acids for the detection of defects of fatty acid oxidation in intact cultured fibroblasts. *J. Inherit. Metab. Dis.* **13,** 58–68
18. Bergmeyer, H. U., Bergmeyer, J., and Grassl, M. (1986) *Methods of Enzymatic Analysis*, Vol. 2, 3rd ed., VCH Verslagsgesellschaft mbH, Weinheim, Germany
19. Ramakers, C., Ruijter, J. M., Deprez, R. H., and Moorman, A. F. (2003) Assumption-free analysis of quantitative real-time polymerase chain reaction (PCR) data. *Neurosci. Lett.* **339,** 62–66
20. Van Vlies, N., Ruiter, J. P., Doolaard, M., Wanders, R. J., and Vaz, F. M. (2007) An improved enzyme assay for carnitine palmitoyl transferase I in fibroblasts using tandem mass spectrometry. *Mol. Genet. Metab.* **90,** 24–29
21. IJlst, L., Mandel, H., Oostheim, W., Ruiter, J. P., Gutman, A., and Wanders, R. J. (1998) Molecular basis of hepatic carnitine palmitoyltransferase I deficiency. *J. Clin. Invest.* **102,** 527–531
22. Minkler, P. E., Stoll, M. S., Ingalls, S. T., Yang, S., Kerner, J., and Hoppel, C. L. (2008) Quantification of carnitine and acylcarnitines in biological matrices by HPLC electrospray ionization-mass spectrometry. *Clin. Chem.* **54,** 1451–1462
23. Minkler, P. E., Stoll, M. S., Ingalls, S. T., and Hoppel, C. L. (2011) *J. Am. Soc. Mass Spectrom.* **22**(Suppl. 1), 69 (poster abstract)
24. Brendel, K., and Bressler, R. (1967) The resolution of (plus or minus)-carnitine and the synthesis of acylcarnitines. *Biochim. Biophys. Acta* **137,** 98–106
25. Wanders, R. J., Kos, M., Roest, B., Meijer, A. J., Schrakamp, G., Heymans, H. S., Tegelaers, W. H., van den Bosch, H., Schutgens, R. B., and Tager, J. M. (1984) Activity of peroxisomal enzymes and intracellular distribution of catalase in Zellweger syndrome. *Biochem. Biophys. Res. Commun.* **123,** 1054–1061
26. Wanders, R. J., van Roermund, C. W., de Vries, C. T., van den Bosch, H., Schrakamp, G., Tager, J. M., Schram, A. W., and Schutgens, R. B. (1986) Peroxisomal beta-oxidation of palmitoyl-CoA in human liver homogenates and its deficiency in the cerebro-hepato-renal (Zellweger) syndrome. *Clin. Chim. Acta* **159,** 1–10
27. Bradford, M. M. (1976) A rapid and sensitive method for the quantitation of microgram quantities of protein utilizing the principle of protein-dye binding. *Anal. Biochem.* **72,** 248–254
28. Zhang, D., Yu, W., Geisbrecht, B. V., Gould, S. J., Sprecher, H., and Schulz, H. (2002) Functional characterization of Delta3,Delta2-enoyl-CoA isomerases from rat liver. *J. Biol. Chem.* **277,** 9127–9132
29. Kurtz, D. M., Rinaldo, P., Rhead, W. J., Tian, L., Millington, D. S., Vockley, J., Hamm, D. A., Brix, A. E., Lindsey, J. R., Pinkert, C. A., O'Brien, W. E., and Wood, P. A. (1998) Targeted disruption of mouse long-chain acyl-CoA dehydrogenase gene reveals crucial roles for fatty acid oxidation. *Proc. Natl. Acad. Sci. U. S. A.* **95,** 15592–15597
30. Cox, K. B., Hamm, D. A., Millington, D. S., Matern, D., Vockley, J., Rinaldo, P., Pinkert, C. A., Rhead, W. J., Lindsey, J. R., and Wood, P. A. (2001) Gestational, pathologic and biochemical differences between very long-chain acyl-CoA dehydrogenase deficiency and long-chain acyl-CoA dehydrogenase deficiency in the mouse. *Hum. Mol. Genet.* **10,** 2069–2077
31. Bakermans, A. J., Geraedts, T. R., van Weeghel, M., Denis, S., Joao Ferraz, M., Aerts, J. M., Aten, J., Nicolay, K., Houten, S. M., and Prompers, J. J. (2011) Fasting-induced myocardial lipid accumulation in long-chain acyl-CoA dehydrogenase knockout mice is accompanied by impaired left ventricular function. *Circ. Cardiovasc. Imaging* **4,** 558–565
32. Miinalainen, I. J., Schmitz, W., Huotari, A., Autio, K. J., Soininen, R., Ver Loren van Themaat, E., Baes, M., Herzig, K.-H., Conzelmann, E., and Hiltunen, J. K. (2009) Mitochondrial 2,4-dienoyl-CoA reductase deficiency in mice results in severe hypoglycemia with stress intolerance and unimpaired ketogenesis. *PLoS Genet.* **5,** e1000543

Received for publication February 29, 2012.
Accepted for publication June 20, 2012.